DEUTSCHES ELEKTRONEN-SYNCHROTRON DESY

DESY 79/36
July 1979

HADRON FINAL STATES IN THE TASSO DETECTOR AT PETRA

by

D. Notz

NOTKESTRASSE 85 · 2 HAMBURG 52

To be sure that your preprints are promptly included in the
HIGH ENERGY PHYSICS INDEX ,
send them to the following address (if possible by air mail) :

DESY
Bibliothek
Notkestrasse 85
2 Hamburg 52
Germany

Two-Particle Correlations in e^+e^- Jets from QCD

by

G. Schierholz and J. Willrodt
II. Institut für Theoretische Physik der Universität Hamburg

Abstract

Two-particle correlation functions are introduced which vanish in the naive quark-parton model (zeroth order QCD) and directly measure higher order QCD corrections, i. e., three- (or more) jet final states. They have the advantage over a multi-jet analysis in spherocity, thrust and acoplanarity (i) to be insensitive to heavy quark-antiquark pair production and (ii) to be easy to measure. Detailed predictions for two-particle correlations are presented.

(Submitted to Zeitschr. f. Physik C)

1. Introduction

Quantum chromodynamics (QCD) predicts a multi-jet structure of the hadronic final states in e^+e^- annihilation[1]. Besides the predominant two-jet events, three-jet final states associated with $q\bar{q}g$ production are expected at a rate of 15 - 20 % for $\sqrt{q^2} \gtrsim 20$ GeV while four-jet events due to $q\bar{q}gg$ production will contribute a notable ~ 5 % to the total cross section[2].

At first sight, the multi-jet structure will manifest itself in a nonvanishing[2,3] $\langle S \rangle$, $\langle 1-T \rangle$ and $\langle A \rangle$ (S, T, A being spherocity[4], thrust[5] and acoplanarity[6], respectively) and a rising averaged[7,8] $\langle p_T^2 \rangle$ (with q^2). Beyond, perturbative QCD makes definite predictions for the differential and doubly differential cross sections in spherocity, thrust and acoplanarity[2,3] as well as for angular correlations of jet axes[8,9] (event topologies).

In the presence of heavy quark-antiquark ($Q\bar{Q}$) pair production, quantitative QCD tests on the level of spherocity, thrust and acoplanarity distributions will, however, be made very difficult. The reason is that (heavy) $Q\bar{Q}$ production will also give rise to events with $\langle S \rangle$, $\langle 1-T \rangle$ and $\langle A \rangle$ much larger than the non-perturbative light quark background[10] which are hard to distinguish from QCD multi-jet final states. Just above threshold, those events are expected to be almost spherical while for larger q^2 we find $\langle S \rangle, \langle A \rangle \approx 4\, m_Q^2/q^2$ and $\langle 1-T \rangle \approx (\pi/4)\, m_Q/\sqrt{q^2}$.

The multi-jet structure of the hadronic final states will, likewise, express itself in the one- and two-particle inclusive distributions. The fact that this involves the gluon fragmentation function as an unknown is rather a positive feature as it will give answer to such important questions like: is the gluon jet flavour neutral? QCD predictions on the level of one- and two-particle inclusive distributions seem to be less sensitive to the aforementioned heavy quark-antiquark pair production background. For example, the mean p_T^2 of hadrons which peaks around[7,11] $x \approx 0.5$ (with peak value $\sim \alpha_s(q^2)\, q^2$, seagull effect) is found to be essentially not effected since the cross section involving heavy quark production clusters around[12] $x \lesssim 0.2$. Another fine example will be stated below.

In this paper we shall consider the two-particle inclusive cross section to order α_s. Since we are primarily interested in the primordial jet production

mechanism, we shall concentrate on opposite hemisphere correlations - opposite with respect to the plane perpendicular to the thrust axis and going through the origin of the event. This avoids short-range correlations of particles within the same jet which fall into the domain of nonperturbative QCD and, by nature, we do not know much about. More precisely, we shall be dealing with the correlation function

$$C^{cc}(x_1,x_2) = \left(\frac{1}{\sigma}\frac{d^2\sigma^{cc}}{dx_1\,dx_2}\right)_{\substack{\text{opposite}\\ \text{hemisphere}}} - \frac{1}{2}\,\frac{1}{\sigma}\frac{d\sigma^c}{dx_1}\,\frac{1}{\sigma}\frac{d\sigma^c}{dx_2}\,, \tag{1.1}$$

where it is summed over all charged particles (indicated by c). This receives contributions only from order α_s (i. e., three-jet final states) and higher and vanishes in the naive quark-parton model[+] which makes (1.1) an interesting quantity for testing QCD.

In Section 2 we shall deal with massless quarks. We calculate $C^{cc}(x_1,x_2)$ and show that it is infrared finite by itself (which saves us the infrared "renormalization"). In Section 3 massive quarks are taken into consideration. In this case (1.1) also receives contributions from zeroth order. By taking the energy weighted average over, say, particle 2, the zeroth order contribution drops out again which brings us back into the fortunate situation where a nonvanishing correlation indicates a three-jet (or higher) final state. Finally, in Section 4 we make some concluding remarks.

2. Massless Quarks

Let us first consider the case where all quark masses are zero or can be neglected. In the (hypothetical) case of zero or equal quark masses, the (total) fragmentation functions summed over all (e. g., charged) particles will be identical for the various species,

$$D_u^c = D_d^c = D_s^c = D_c^c = D_b^c = \cdots\cdots\,, \tag{2.1}$$

[+] For all quark masses being zero; see later on.

in correspondence with $SU(N_f)$ symmetry. For realistic quark masses, (2.1) will be approached only for very large q^2 far above any (heavy) $Q\bar{Q}$ production threshold, but surely it will be approached as a result of the evolution equations[13]. We have, however, no idea how fast this approach will be.

Writing

$$\mathcal{D}_q^c = \mathcal{D}_u^c = \mathcal{D}_d^c = \cdots\cdots \tag{2.2}$$

and noticing that $\mathcal{D}_q^c = \mathcal{D}_{\bar{q}}^c$, we find in zeroth order QCD$^+$ (naive quark-parton model)

$$\begin{aligned} C^{cc}(x_1, x_2) &= \left[\mathcal{D}_q^c(x_1)\mathcal{D}_{\bar{q}}^c(x_2) + \mathcal{D}_{\bar{q}}^c(x_1)\mathcal{D}_q^c(x_2) \right] \\ &\quad - \frac{1}{2}\left(\mathcal{D}_q^c(x_1) + \mathcal{D}_{\bar{q}}^c(x_1)\right)\left(\mathcal{D}_q^c(x_2) + \mathcal{D}_{\bar{q}}^c(x_2)\right) \\ &= 0 \quad , \end{aligned} \tag{2.3}$$

where the first term in square brackets represents

$$\left(\frac{1}{\sigma}\,\frac{d^2\sigma^{cc}}{dx_1\,dx_2}\right)_{\substack{\text{opposite}\\ \text{hemisphere}}} . \tag{2.4}$$

This is understood to be the cross section for finding a hadron with fractional momentum x_1 in either one jet (hemisphere) and a hadron with fractional momentum x_2 in the respective opposite jet (hemisphere). It is always assumed that the nonperturbative jet-spread is negligibly small. In practice, x_1 and x_2 should, however, not be taken infinitesimally small ($x_1, x_2 \gg 2\langle p_T\rangle_{\text{nonpert.}}/\sqrt{q^2}$) as the quark-parton model does not apply here anymore.

+ We shall drop the q^2-dependence from the argument of the fragmentation functions.

The fact that $C^{cc}(x_1,x_2)$ vanishes in zeroth order perturbation theory means that the quark-antiquark two-jet final state factorizes when summed over all charged particles. Similarly, we find

$$C^{cn} = C^{nc} = C^{nn} = 0 \,, \tag{2.5}$$

where n stands for the sum over all neutral particles. In higher order in α_s we expect $C^{cc}(x_1,x_2)$ to be nonzero due to kinematically correlated quark, antiquark and gluon jets, so that a nonvanishing correlation function is a characteristic feature of QCD.

In second order perturbation theory (2.4) receives contributions from the $(q\bar{q}g)$ three-jet final state as well as from the vertex graph interfering with the Born diagram (fig. 1). The vertex diagram (fig. 1b), being divergent by itself, functions as a regulator of the infrared and collinear singularities inherent in the three-jet diagram, while diagrams 1a contain the physics.

Since the thrust axis coincides with the direction of the most energetic jet, one of the two hadrons must originate in the fastest parton. In fig. 2 we have schematically drawn the parton content of the two-particle inclusive cross section (2.4). This divides the events into three main classes. Defining

$$x_q = \frac{2p_q}{\sqrt{q^2}} \,, \quad x_{\bar{q}} = \frac{2p_{\bar{q}}}{\sqrt{q^2}} \,, \quad x_g = \frac{2p_g}{\sqrt{q^2}} \,, \quad x_q + x_{\bar{q}} + x_g = 2 \,, \tag{2.6}$$

we distinguish between[+]:

I:	$x_q > x_{\bar{q}}, x_g$	quark most energetic	
II:	$x_{\bar{q}} > x_q, x_g$	antiquark most energetic	(2.7)
III:	$x_g > x_q, x_{\bar{q}}$	gluon most energetic	

The kinematic boundaries of the three regions are shown in fig. 3.

[+] See also ref. 9.

Collecting now the various contributions according to fig. 2 we obtain:

$$
\begin{aligned}
C^{cc}(x_1,x_2) = \frac{2}{3}\frac{\alpha_s}{\pi}\Bigg[& \underset{I+II}{\int_{x_1}^{1}\frac{dx_q}{x_q}\int_{x_2}^{1}\frac{dx_{\bar q}}{x_{\bar q}}} K\, D_q^c\!\left(\tfrac{x_1}{x_q}\right) D_{\bar q}^c\!\left(\tfrac{x_2}{x_{\bar q}}\right) \\
& + \underset{I+III}{\int_{x_1}^{1}\frac{dx_q}{x_q}\int_{x_2}^{1}\frac{dx_g}{x_g}} K\, D_q^c\!\left(\tfrac{x_1}{x_q}\right) D_g^c\!\left(\tfrac{x_2}{x_g}\right) \\
& + \underset{II+III}{\int_{x_1}^{1}\frac{dx_g}{x_g}\int_{x_2}^{1}\frac{dx_{\bar q}}{x_{\bar q}}} K\, D_g^c\!\left(\tfrac{x_1}{x_g}\right) D_{\bar q}^c\!\left(\tfrac{x_2}{x_{\bar q}}\right) \\
& - D_q^c(x_1)\underset{I+II+III}{\int_0^1 dx_q\int_{x_2}^{1}\frac{dx_{\bar q}}{x_{\bar q}}} K\, D_{\bar q}^c\!\left(\tfrac{x_2}{x_{\bar q}}\right) \\
& - D_{\bar q}^c(x_2)\underset{I+II+III}{\int_{x_1}^{1}\frac{dx_q}{x_q}\int_0^1 dx_{\bar q}} K\, D_q^c\!\left(\tfrac{x_1}{x_q}\right) \\
& - D_q^c(x_1)\underset{I+II+III}{\int_0^1 dx_q\int_{x_2}^{1}\frac{dx_g}{x_g}} K\, D_g^c\!\left(\tfrac{x_2}{x_g}\right) \\
& + D_q^c(x_1)\, D_{\bar q}^c(x_2)\underset{I+II+III}{\int_0^1 dx_q\int_0^1 dx_{\bar q}} K \Bigg] \\
& + (x_1 \longleftrightarrow x_2)\,,
\end{aligned}
\tag{2.8}
$$

where[3,9]

$$K = \frac{x_q^2 + x_{\bar{q}}^2}{(1-x_q)(1-x_{\bar{q}})} \quad . \tag{2.9}$$

The vertex diagram (fig. 1b) does not appear explicitly. We have made use of the relation

$$+ \frac{2}{3}\frac{\alpha_s}{\pi}\int_0^1 dx_q \int_0^1 dx_{\bar{q}}\, K = \frac{\alpha_s}{\pi} \quad . \tag{2.10}$$

$I + II + III$

The first three integrals in (2.8) extend only over a limited region of phase space according to the three classes of events indicated in fig. 2. The actual phase space is stated under the integrals. Note that the full phase space corresponds to regions I + II + III.

Equation (2.8) is infrared finite, though separately the various contributions are not. The infrared and collinear singularities cancel which means that we need not go through the procedure of infrared "renormalization". Equation (2.8) can be rewritten in a form which explicitely reveals its infrared finiteness:

$$C^{CC}(x_1,x_2) = \frac{2}{3}\frac{\alpha_s}{\pi}\Bigg[\underbrace{\int_{x_1}^1 \frac{dx_q}{x_q}\int_{x_2}^1 \frac{dx_{\bar{q}}}{x_{\bar{q}}}\, K\left(\mathcal{D}_q^c\left(\tfrac{x_1}{x_q}\right) - x_q \mathcal{D}_q^c(x_1)\right)\left(\mathcal{D}_{\bar{q}}^c\left(\tfrac{x_2}{x_{\bar{q}}}\right) - x_{\bar{q}} \mathcal{D}_{\bar{q}}^c(x_2)\right)}_{I+II}$$

$$+ \underbrace{\int_{x_1}^1 \frac{dx_q}{x_q}\int_{x_2}^1 \frac{dx_g}{x_g}\, K\left(\mathcal{D}_q^c\left(\tfrac{x_1}{x_q}\right) - x_q \mathcal{D}_q^c(x_1)\right)\mathcal{D}_g^c\left(\tfrac{x_2}{x_g}\right)}_{I+III}$$

$$+ \int_{x_1}^{1} \frac{dx_g}{x_g} \int_{x_2}^{1} \frac{dx_{\bar{q}}}{x_{\bar{q}}} K \, \mathcal{D}_g^c\left(\frac{x_1}{x_g}\right)\left(\mathcal{D}_{\bar{q}}^c\left(\frac{x_2}{x_{\bar{q}}}\right) - x_{\bar{q}}\,\mathcal{D}_{\bar{q}}^c(x_2)\right)$$

II + III

$$- \mathcal{D}_q^c(x_1) \int_0^{x_1} dx_q \int_{x_2}^{1} \frac{dx_{\bar{q}}}{x_{\bar{q}}} K \left(\mathcal{D}_{\bar{q}}^c\left(\frac{x_2}{x_{\bar{q}}}\right) - x_{\bar{q}}\,\mathcal{D}_{\bar{q}}^c(x_2)\right)$$

I + II

$$- \mathcal{D}_{\bar{q}}^c(x_2) \int_{x_1}^{1} \frac{dx_q}{x_q} \int_0^{x_2} dx_{\bar{q}} K \left(\mathcal{D}_q^c\left(\frac{x_1}{x_q}\right) - x_q\,\mathcal{D}_q^c(x_1)\right)$$

I + II

$$- \left(\mathcal{D}_q^c(x_1) + \mathcal{D}_{\bar{q}}^c(x_1)\right) \int_0^{1} dx_q \int_{x_2}^{1} \frac{dx_{\bar{q}}}{x_{\bar{q}}} K \, \mathcal{D}_{\bar{q}}^c\left(\frac{x_2}{x_{\bar{q}}}\right)$$

III

$$- \mathcal{D}_q^c(x_1) \int_0^{x_1} dx_q \int_{x_2}^{1} \frac{dx_g}{x_g} K \, \mathcal{D}_g^c\left(\frac{x_2}{x_g}\right)$$

I + III

$$- \mathcal{D}_{\bar{q}}^c(x_2) \int_{x_1}^{1} \frac{dx_g}{x_g} \int_0^{x_2} dx_{\bar{q}} K \, \mathcal{D}_g^c\left(\frac{x_1}{x_g}\right)$$

II

$$+ \mathcal{D}_q^c(x_1) \int_{x_1}^{1} dx_q \int_{x_2}^{1} \frac{dx_g}{x_g} K \, \mathcal{D}_g^c\left(\frac{x_2}{x_g}\right)$$

III

$$+ \mathcal{D}_q^c(x_1)\,\mathcal{D}_{\bar{q}}^c(x_2) \Big(\underbrace{\int_0^{x_1} dx_q \int_0^{x_2} dx_{\bar{q}}}_{\text{I+II}} + \underbrace{\int_0^{1} dx_q \int_0^{1} dx_{\bar{q}}}_{\text{III}} \Big) K \Big]$$

$$+ (x_1 \longleftrightarrow x_2) \, . \qquad (2.11)$$

The kernel K (eq. (2.9)) becomes singular for $x_q, x_{\bar{q}} \to 1$. Whenever the integration extends to these values, the singularity is cancelled by the zero of, e. g.,

$$\mathcal{J}_q^c\left(\frac{x}{x_q}\right) - x_q \mathcal{J}_q^c(x_1) . \tag{2.12}$$

The limit $x_{q,\bar{q}} \to 1$ corresponds to the case where the internal quark or antiquark goes on mass shell. It is the fact that the two hemispheres factorize for on-mass-shell $q\bar{q}$ production which makes the correlation function $C^{cc}(x_1, x_2)$ infrared finite, similar to the vanishing of the zeroth order contribution.

In table 1 numerical values for the ratio

$$C^{cc}(x_1, x_2) \Big/ \mathcal{J}_q^c(x_1)\, \mathcal{J}_{\bar{q}}^c(x_2) \tag{2.13}$$

are given for various x_1, x_2, where we have taken

$$\mathcal{J}_q^c(x) = 2\, \frac{(1-x)^2}{x} \tag{2.14}$$

and

$$A: \quad \mathcal{J}_g^c(x) = \int_x^1 \frac{dx_q}{x_q}\, \mathcal{J}_q^c\left(\frac{x}{x_q}\right) + \int_x^1 \frac{dx_{\bar{q}}}{x_{\bar{q}}}\, \mathcal{J}_{\bar{q}}^c\left(\frac{x}{x_{\bar{q}}}\right)$$

$$= 4\, \frac{1-x^2}{x} + 8 \ln x \tag{2.15}$$

$$B: \quad \mathcal{J}_g^c(x) = \mathcal{J}_q^c(x) = 2\, \frac{(1-x)^2}{x} . \tag{2.16}$$

Choice A corresponds to the case where the gluon fragments first into a quark and antiquark, respectively, with a flat momentum distribution[14] which then decay with fragmentation function (2.14). Choice A is somewhat softer than choice B. All fragmentation functions are normalized to

$$\int_0^1 dx\, x\, \mathcal{D}^c(x) = \frac{2}{3} \tag{2.17}$$

which, however, cancels out in (2.13). In fig. 4 (2.13) is shown graphically. The triangle $x_2 > x_1$ which is the mirror image of $x_1 > x_2$ has been left out for better view. The figures given correspond to $\alpha_s = 0.25$ (which is equivalent to $\sqrt{q^2} = 20$ GeV, $\Lambda = 0.7$ GeV, $N_f = 5$).

The correlation predicted is quite large. For medium x_1, x_2 where one can expect sufficient statistics, it reaches the level of[+] ~ 20 %. The effect is largest for $x_1, x_2 \to 1$. Here it also depends critically on the choice of the gluon fragmentation function, while for medium x_1, x_2 choice A and B differ by not more than 10 %.

3. Nonasymptotic Region

For nonasymptotic q^2, where quark masses cannot be neglected, the (total inclusive) light and heavy quark fragmentation functions will generally be different. This means that, in the presence of heavy quarks, $C^{cc}(x_1, x_2)$ will not vanish anymore in zeroth order.

Assuming that there are only two types of quarks, one light and one heavy, with fragmentation functions $\mathcal{D}_q$ and $\mathcal{D}_Q$ and charges Q_q and Q_Q, we obtain in zeroth order (naive quark-parton model)

[+] Based on the normalization (2.13).

$$C^{cc}(x_1,x_2) = \frac{2Q_q^2Q_Q^2}{(Q_q^2+Q_Q^2)^2}\left(\mathcal{D}_q^c(x_1)-\mathcal{D}_Q^c(x_1)\right) \times \left(\mathcal{D}_{\bar{q}}^c(x_2)-\mathcal{D}_{\bar{Q}}^c(x_2)\right) \quad , \tag{3.1}$$

and similarly for the more realistic case of several light and heavy quarks. Only for very large q^2 (far above $4m_Q^2$) can we expect (3.1) to vanish, i. e.,

$$\mathcal{D}_Q^c(x) \longrightarrow \mathcal{D}_q^c(x) . \tag{3.2}$$

This means that a nonvanishing correlation function $C^{cc}(x_1,x_2)$ is not confidently a signature of QCD. However, the zeroth order contribution is rather small. If we allow $\mathcal{D}_q^c$ and $\mathcal{D}_Q^c$ to differ by 20 %, expression (3.1) gives a 2 % (1.3 %) contribution to (2.13) for equal (different) charges. This is to be compared to, say, a 20 % effect coming from second order perturbation theory[+].

The non-QCD background (3.1) can be fully eliminated by summing, e. g., over the energy in the jet opposite to particle 1:

$$\int_0^1 dx_2\, x_2 \left(\mathcal{D}_q^c(x_1)-\mathcal{D}_Q^c(x_1)\right)\left(\mathcal{D}_{\bar{q}}^c(x_2)-\mathcal{D}_{\bar{Q}}^c(x_2)\right) = 0 \tag{3.3}$$

as a matter of the normalization condition[++] (2.17). This gives the desired result

---

[+] The error one makes by neglecting (3.1) is certainly smaller than the uncertainties accompanying $\mathcal{D}_q^c(x)$ and $\mathcal{D}_{\bar{q}}^c(x)$.

[++] To be precise, energy conservation only tells us that $\int_0^1 dx\, x\, \mathcal{D}^{c+n}(x) = 1$, and we may well have $\int_0^1 dx\, x\, \mathcal{D}_q^c(x) \neq \int_0^1 dx\, x\, \mathcal{D}_Q^c(x)$. So, generally (3.3) is only true if it is summed over charged and neutral energy (i. e., for $C^{c,c+n}(x_1,x_2)$). If necessary the reader should place the obvious changes.

$$\int_0^1 dx_2\, x_2\, C^{cc}(x_1,x_2) = O(\alpha_s) \tag{3.4}$$

which, being nonzero, constitutes a genuine signal of QCD now. By $D_q^c(x)$ we shall understand now the average of light and heavy quark fragmentation functions[+] and leave out the quark masses in the $q\bar{q}g$-production amplitudes. We then obtain from eq. (2.11):

$$\begin{aligned}
\int_0^1 dx_2\, x_2\, C^{cc}(x_1,x_2) = \frac{4}{9}\frac{\alpha_s}{\pi}\Bigg[& 2\int_{x_1}^1 \frac{dx_q}{x_q}\int_0^1 dx_{\bar{q}}\,(1-x_q)\,K\left(D_q^c\left(\frac{x_1}{x_q}\right)-x_q D_q^c(x_1)\right) \qquad \text{I} \\
& - 2\int_{x_1}^1 \frac{dx_{\bar{q}}}{x_{\bar{q}}}\int_0^1 dx_q\,(1-x_q)\,K\left(D_{\bar{q}}^c\left(\frac{x_1}{x_{\bar{q}}}\right)-x_{\bar{q}} D_{\bar{q}}^c(x_1)\right) \qquad \text{I} \\
& - 2\int_{x_1}^1 \frac{dx_q}{x_q}\int_0^1 dx_{\bar{q}}\,(1-x_q)\,K\, D_q^c\left(\frac{x_1}{x_q}\right) \qquad \text{III} \\
& - \int_{x_1}^1 \frac{dx_g}{x_g}\int_0^1 dx_q\,(1-x_g)\,K\, D_g^c\left(\frac{x_1}{x_g}\right) \qquad \text{III} \\
& - 2\int_{x_1}^1 \frac{dx_g}{x_g}\int_0^1 dx_q\,(1-x_q)\,K\, D_g^c\left(\frac{x_1}{x_g}\right) \qquad \text{I} \\
& - 2\, D_q^c(x_1)\int_0^{x_1} dx_q\int_0^1 dx_{\bar{q}}\,(1-x_q)\,K \qquad \text{I}
\end{aligned}$$

[+] Weighted by their charge squared.

$$+ 2\, \mathcal{D}_{\bar{q}}^{c}(x_1) \int_0^{x_1} dx_{\bar{q}} \int_0^1 dx_q\, (1-x_q)\, K \Big]_{,} \qquad (3.5)$$

where we have made use of the normalization condition (2.17). As can easily be checked, the various integrals in (3.5) are all infrared finite.

From fig. 4 we gather that a great portion of the correlation will cancel when integrating out one particle due to the fact that (2.11) changes sign. In fig. 5 we have plotted

$$\int_0^1 dx_2\, x_2\, C^{cc}(x_1, x_2) \Big/ \mathcal{D}_q^{c}(x_1) \qquad (3.6)$$

for gluon fragmentation functions A and B. The correlation is found to be largest for small x_1 and around $x_1 \approx 0.7$. At maximum it is of the order of ~ 5 %. Choice A and B differ by less than 20 % near their maximum. A somewhat diminished signal (as compared to the full correlation (2.13)) is the price one has to pay for having eliminated the heavy quark background completely.

Taking the energy weighted average over both jets eliminates quark and gluon fragmentation functions totally and brings us close to the energy correlations considered by the Seattle group[15]. This correlation will be further diminished due to the change of sign of (3.6) (cf.fig. 5) which again causes a large cancellation. We obtain

$$\frac{\langle E_1^c E_2^c \rangle_{\substack{\text{opposite} \\ \text{hemisphere}}} - \frac{1}{2}\langle E_1^c \rangle \langle E_2^c \rangle}{\frac{1}{2}\langle E_1^c \rangle \langle E_2^c \rangle} = \left[\int_0^1 dx_1 x_1 \int_0^1 dx_2 x_2\, C^{cc}(x_1, x_2) \right] \times \left[\frac{1}{2} \int_0^1 dx_1 x_1 \frac{1}{\sigma} \frac{d\sigma^c}{dx_1} \int_0^1 dx_2 x_2 \frac{1}{\sigma} \frac{d\sigma^c}{dx_2} \right]^{-1}$$

$$= -\frac{2}{3}\frac{\alpha_s}{\pi}\Bigg[2\underbrace{\int_0^1 dx_q \int_0^1 dx_{\bar{q}}\ \frac{1-x_q}{1-x_{\bar{q}}}\ (x_q^2+x_{\bar{q}}^2)}_{\text{I}} + \underbrace{\int_0^1 dx_q \int_0^1 dx_{\bar{q}}\ (1-x_g)^2\ \frac{x_q^2+x_{\bar{q}}^2}{(1-x_q)(1-x_{\bar{q}})}}_{\text{III}}\Bigg]$$

$$= -\ 0.10\ \frac{\alpha_s}{\pi} \tag{3.7}$$

which is a tiny effect (0.8 % for $\alpha_s = 0.25$) as compared to (2.13) and (3.6).

4. Conclusions

We have seen that QCD predicts sizable two-particle correlations. If one restricts the analysis to faster particles, what one anyway would do because the correlations are largest for more energetic particles, there should be no doubt which particle belongs to which hemisphere. Probably, one will not even have to determine the thrust axis. This means that the two-particle correlations are straightforward to determine experimentally.

The fact that the gluon is flavour neutral was only implicitly made use of. In order to test gluon quantum numbers explicitly one will have to look for two-particle correlations of definite charge. This will be done elsewhere[16].

References

1) J. Ellis, M.K. Gaillard and G. Ross, Nucl. Phys. B111 (1976) 253;
G. Sterman and S. Weinberg, Phys. Rev. Letters 39 (1977) 1436;
A.V. Smilga, Phys. Letters 83B (1979) 357

2) A. Ali, J.G. Körner, Z. Kunszt, J. Willrodt, G. Kramer, G. Schierholz and E. Pietarinen, Phys. Letters 82B (1979) 285

3) A. De Rujula, J. Ellis, E.G. Floratos and M.K. Gaillard, Nucl. Phys. B138 (1978) 387

4) H. Georgi and G. Machacek, Phys. Rev. Letters 39 (1977) 1237

5) E. Farhi, Phys. Rev. Letters 39 (1977) 1587

6) H.D. Politzer, Phys. Letters 70B (1977) 430

7) G. Kramer and G. Schierholz, Phys. Letters 82B (1979) 108

8) S.-Y. Pi, R.L. Jaffe and F.E. Low, Phys. Rev. Letters 41 (1978) 142

9) G. Kramer, G. Schierholz and J. Willrodt, Phys. Letters 79B (1978) 249;
erratum ibid. 80B (1979) 433

10) A. Ali, J.G. Körner, G. Kramer and J. Willrodt, Zeitschr. f. Physik C 1 (1979) 203

11) G. Schierholz and J. Willrodt, to be published;
see also: G. Schierholz, invited talk given at the Nordic Particle Physics Meeting, Copenhagen, April 23 - 25, 1979

12) R. Brandelik et al., DESY preprint DESY 79/14 (1979)

13) H. Georgi and H.D. Politzer, Harvard preprint HUTP-77-A071 (1977);
J.F. Owens, Phys. Letters 76B (1978) 85

14) S.J. Brodsky, D.G. Coyne, T.A. De Grand and R.R. Horgan, Phys. Letters 73B (1978) 203;
K. Koller and T.F. Walsh, Phys. Letters 72B (1977) 227

15) C.L. Basham, L.S. Brown, S.D. Ellis and S.T. Love, Phys. Rev. Letters 41 (1978) 1585

16) K. Mursula and G. Schierholz, to be published

Table and Figure Captions

Tab. 1 The (normalized) correlation function (2.13) for
(a) gluon fragmentation function A and
(b) gluon fragmentation function B.

Fig. 1 Second order QCD diagrams:
(a) three-jet production diagram and
(b) vertex diagram interfering with the Born graph.

Fig. 2 The parton content of the two-particle opposite hemisphere inclusive cross section for the quark (I), antiquark (II) and gluon (III) momentum, respectively, defining the thrust axis.

Fig. 3 Regions of phase space. For the definition of I, II and III see text.

Fig. 4 The (normalized) correlation function (2.13) for
(a) gluon fragmentation function A and
(b) gluon fragmentation function B.
One block corresponds to $\Delta x_{1,2} = 0.1$. The triangle $x_2 > x_1$ which is symmetric to $x_1 > x_2$ has been cut away. For the absolute values see table 1.

Fig. 5 The integrated (normalized) correlation function (3.6) for gluon fragmentation functions A and B.

X_2 \ X_1	0.1	0.2	0.3	0.4	0.5	0.6	0.7	0.8	0.9
0.1	-0.003	-0.008	-0.017	-0.024	-0.035	-0.049	-0.068	-0.097	-0.146
0.2	-0.008	-0.0001	0.004	0.007	0.009	0.011	0.012	0.011	0.002
0.3	-0.017	0.004	0.017	0.028	0.038	0.050	0.062	0.073	0.081
0.4	-0.024	0.007	0.028	0.047	0.064	0.081	0.100	0.118	0.137
0.5	-0.035	0.009	0.039	0.064	0.087	0.110	0.133	0.155	0.183
0.6	-0.049	0.011	0.050	0.081	0.110	0.136	0.162	0.188	0.228
0.7	-0.068	0.012	0.062	0.100	0.133	0.162	0.190	0.223	0.275
0.8	-0.097	0.011	0.073	0.118	0.155	0.188	0.223	0.267	0.339
0.9	-0.146	0.002	0.081	0.137	0.183	0.228	0.275	0.339	0.448

Table 1a

0.1	-0.009	-0.010	-0.015	-0.021	-0.031	-0.044	-0.065	-0.095	-0.144
0.2	-0.010	-0.004	-0.001	0.001	0.001	0.001	-0.002	-0.003	-0.002
0.3	-0.015	-0.001	0.009	0.018	0.028	0.038	0.050	0.068	0.100
0.4	-0.021	0.001	0.018	0.036	0.053	0.073	0.098	0.132	0.190
0.5	-0.031	0.001	0.028	0.053	0.080	0.110	0.146	0.196	0.278
0.6	-0.044	0.001	0.038	0.073	0.110	0.150	0.199	0.265	0.372
0.7	-0.065	-0.002	0.050	0.098	0.146	0.199	0.263	0.346	0.483
0.8	-0.095	-0.003	0.068	0.132	0.196	0.265	0.346	0.454	0.628
0.9	-0.144	-0.002	0.100	0.190	0.278	0.372	0.483	0.628	0.862

Table 1b

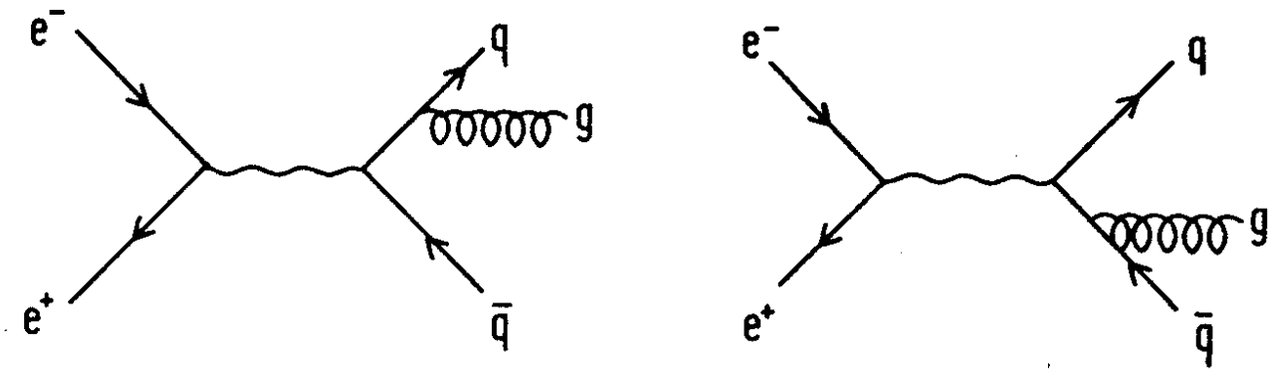

(a)

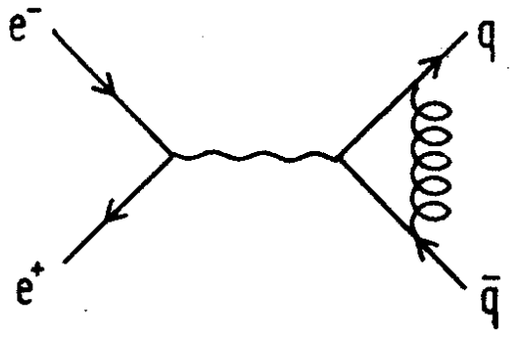

(b)

Fig.1

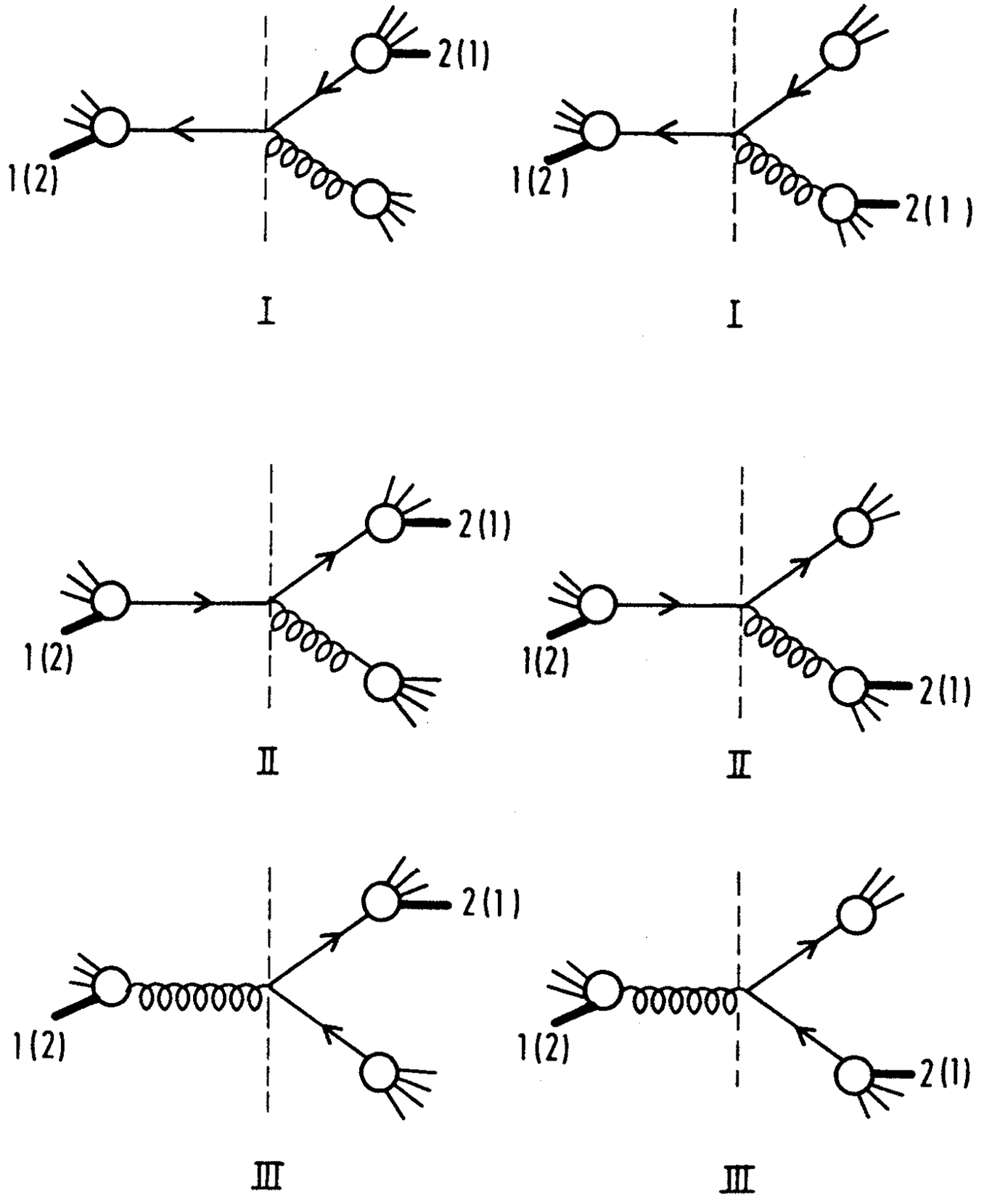

Fig. 2

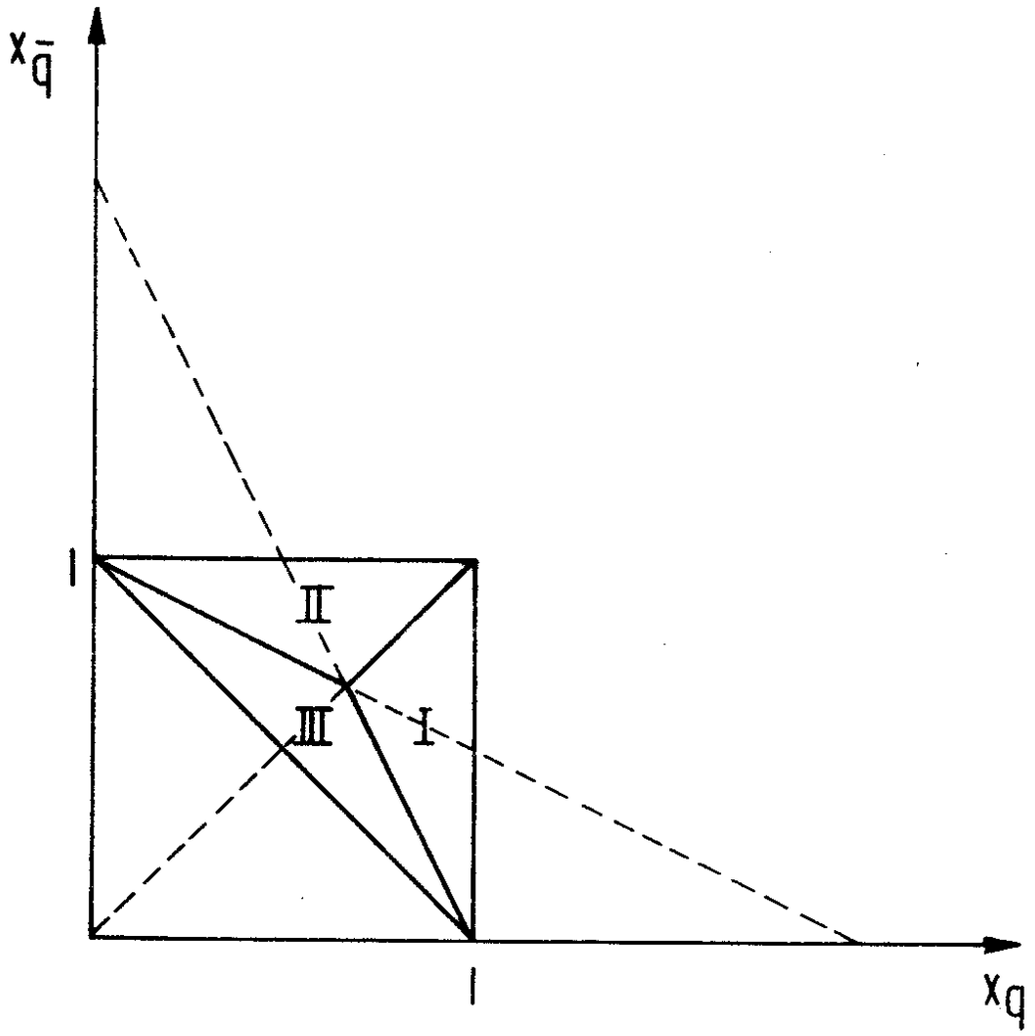

Fig.3

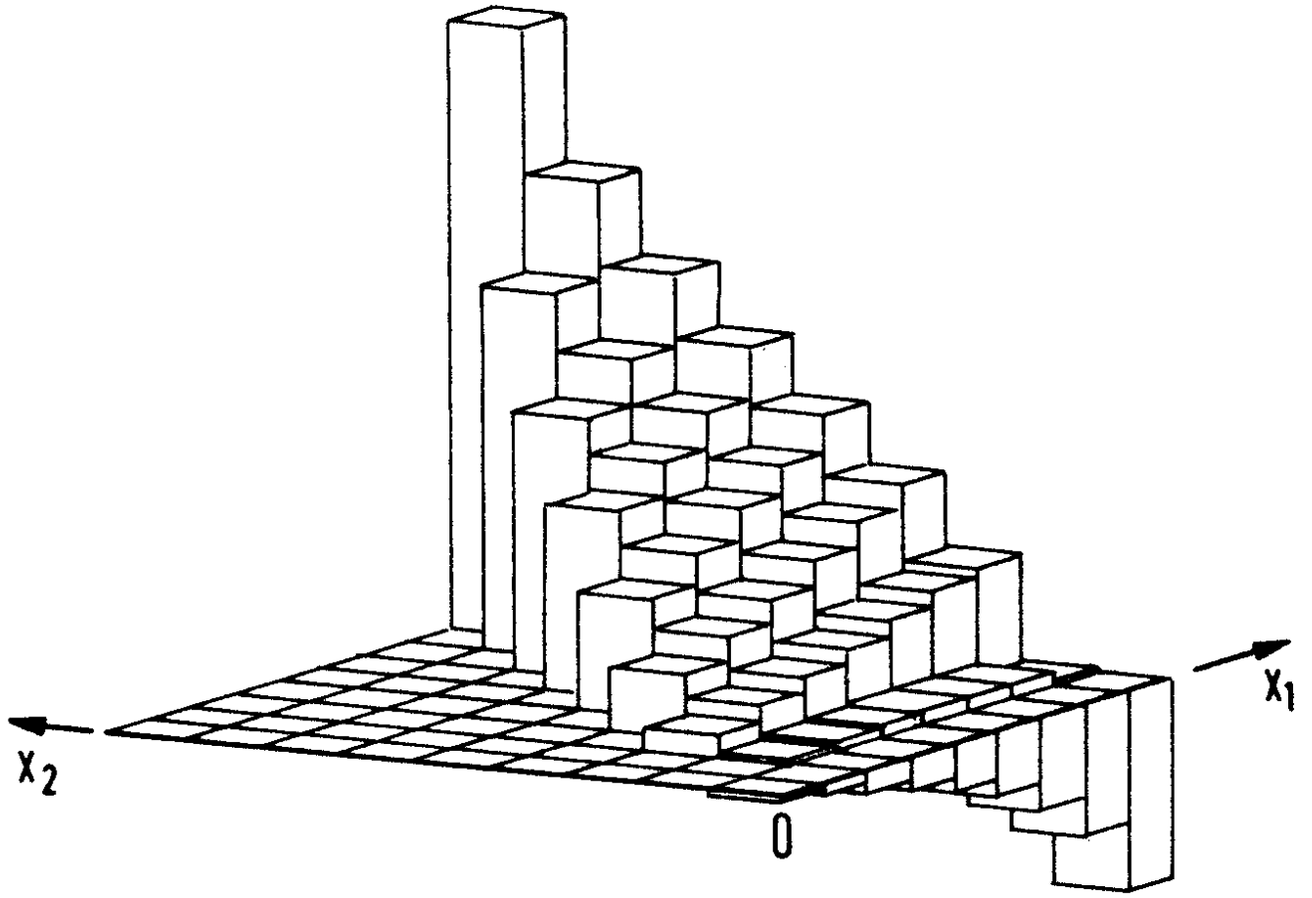

Fig. 4a

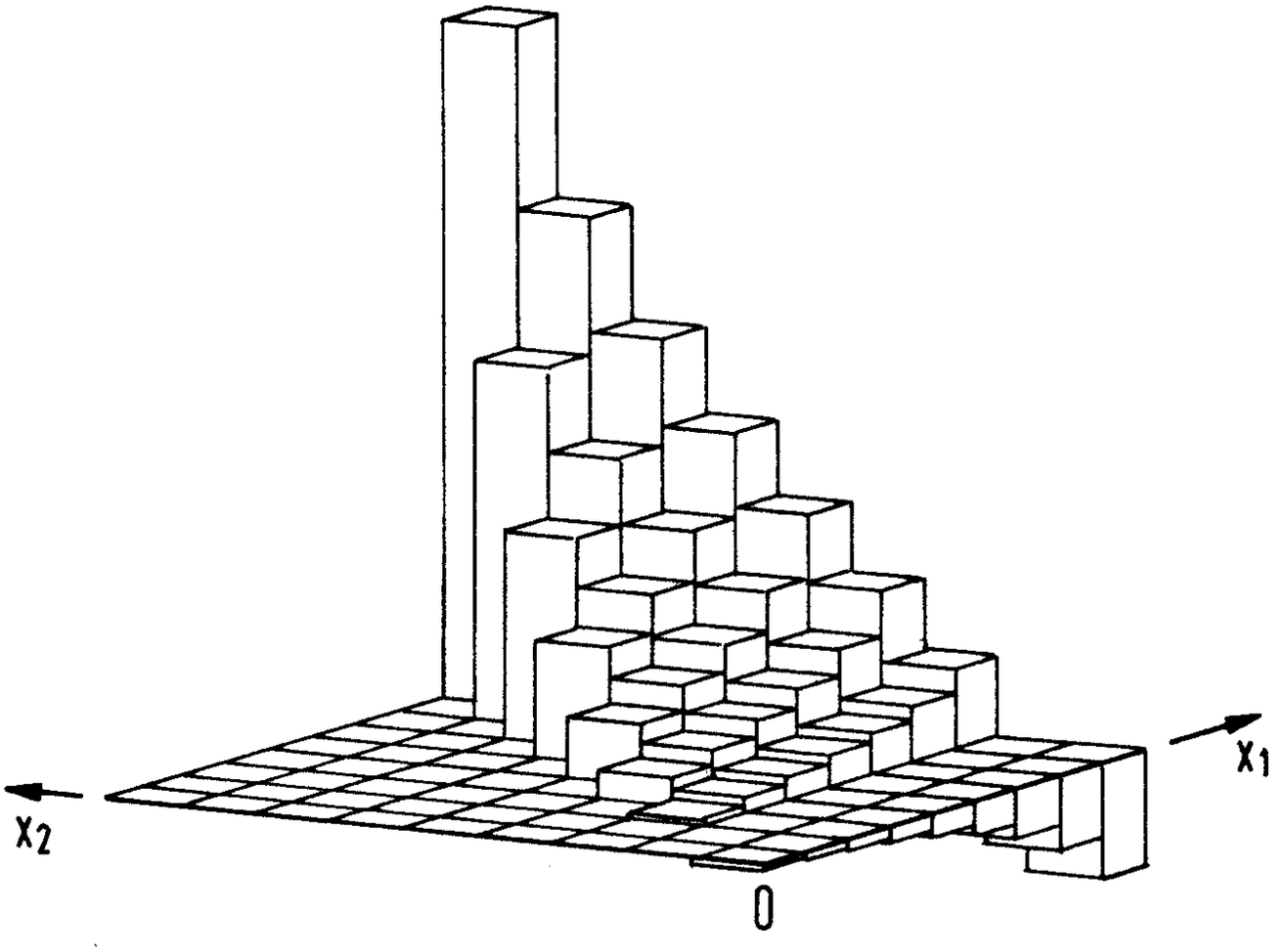

Fig. 4b

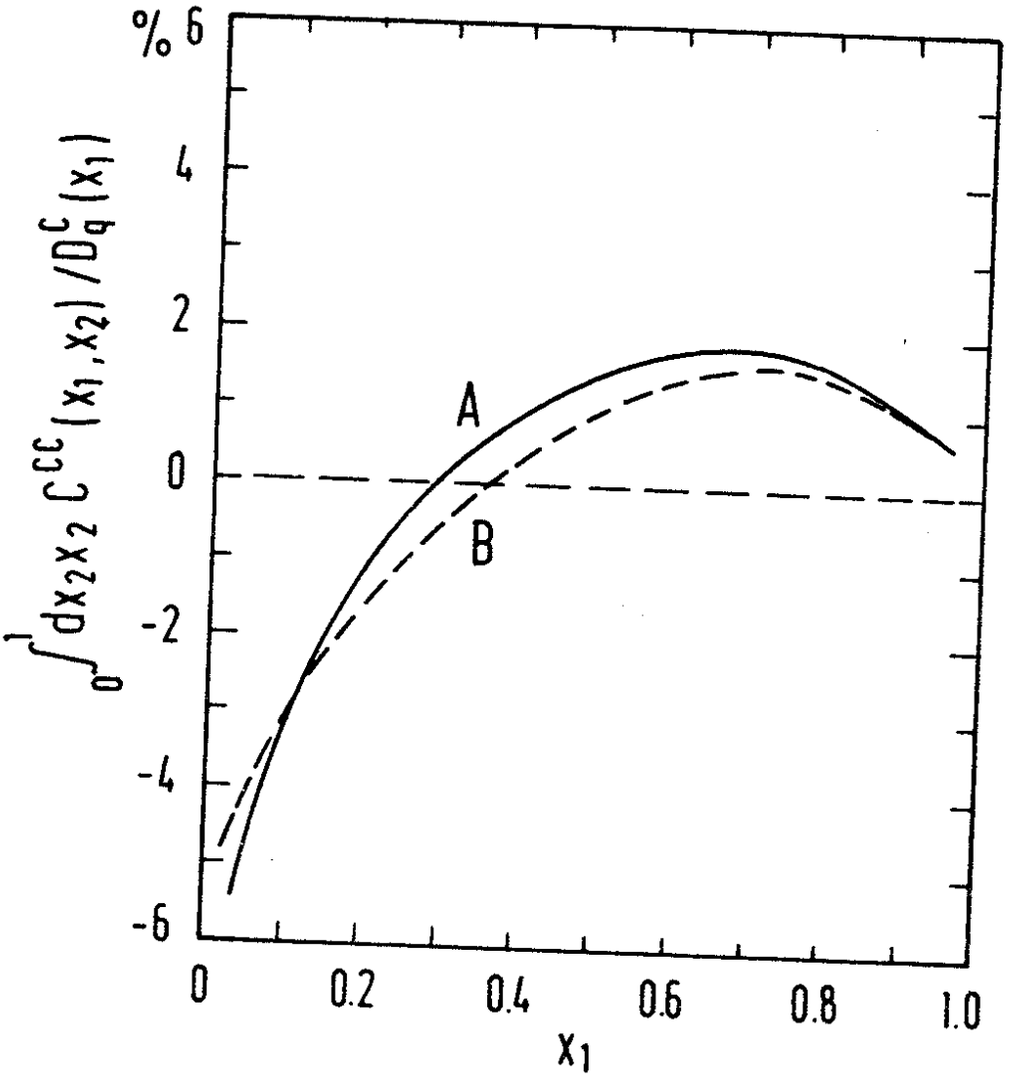

Fig.5